Deletion of a putative HDA-1 binding site in the *hlh-2* promoter eliminates expression in *C. elegans* dorsal uterine cells

Taylor N Medwig-Kinney[1*], Nicholas J Palmisano[1*] and David Q Matus[1§]

[1]Stony Brook University

[§]To whom correspondence should be addressed: david.matus@stonybrook.edu

[*]These authors contributed equally.

Abstract

The helix-loop-helix transcription factor *hlh-2* (E/Daughterless) has been shown to play an important role in regulating cell fate patterning, cell cycle, and basement membrane invasion in the context of the development of the *C. elegans* somatic gonad. Here, using CRISPR/Cas9 genome engineering, we generated a new *hlh-2* allele (*hlh-2(Δ-1303-702)*) in the endogenous, GFP-tagged *hlh-2* locus. This allele represents a deletion of a 601 bp region in the *hlh-2* promoter that contains a putative binding site of the histone deacetylase *hda-1* (HDAC) according to publicly available ChIP-sequencing data. Strikingly, we find that HLH-2 expression is virtually absent in the dorsal uterine cells of *hlh-2(Δ-1303-702)* animals compared to wild type controls. Levels of HLH-2 in the anchor cell and ventral uterine cells are only modestly reduced in the mutant; however, this does not seem to be functionally significant based on the lack of relevant phenotypes and expression levels of a downstream gene, NHR-67 (TLX/Tailless/NR2E1), in these cells. Taken together, these results support growing evidence that HDACs can potentially positively regulate transcription and provide a new reagent for studying *hlh-2* regulation.
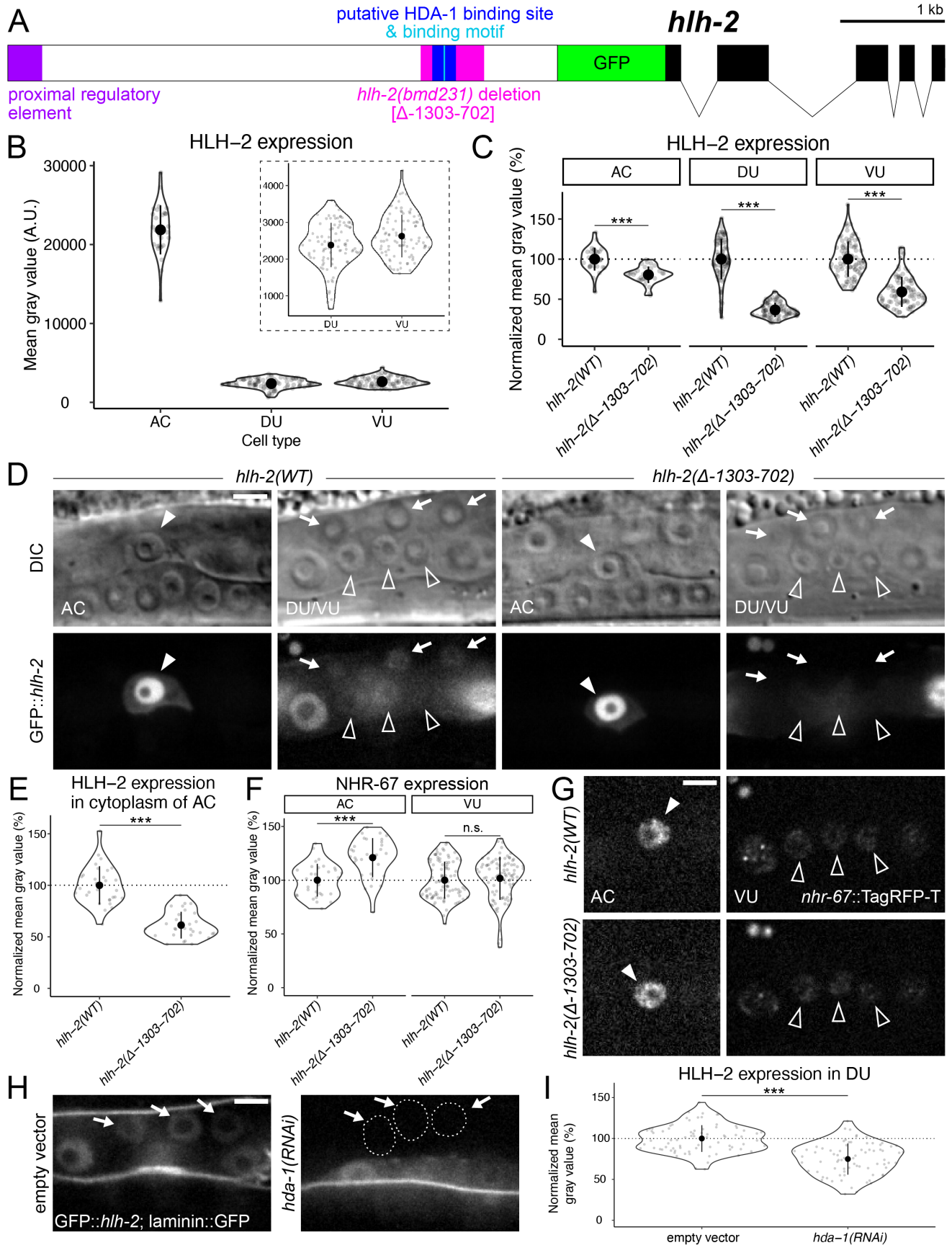
Figure 1. Characterization of new allele deleting putative HDA-1 binding site from the *hlh-2* promoter: (**A**) Schematic of the endogenous GFP::*hlh-2* locus and promoter region, annotated with a previously characterized proximal regulatory element, putative HDA-1 binding site (based on published ChIP-sequencing data) and binding motif, and the genomic region deleted in the *hlh-2(bmd231)* mutant. (**B**) Nuclear expression of wild type (wt) GFP::*hlh-2* in the anchor cell (AC), dorsal uterine (DU) cells, and ventral uterine (VU) cells. (**C-D**) Nuclear expression of GFP::*hlh-2* in the AC (solid arrowhead), DU (arrows), and VU (unfilled arrowheads) cells of *hlh-2(WT)* and *hlh-2(Δ-1303-702)* animals. (**D-E**) Cytoplasmic expression of HLH-2 in the AC of *hlh-2(WT)* and *hlh-2(Δ-1303-702)* animals. (**F-G**) Expression of *nhr-67*::TagRFP-T in *hlh-2(WT)* and *hlh-2(Δ-1303-702)* animals. (**H-I**) Levels of GFP::*hlh-2* following depletion of *hda-1* via RNA interference compared to empty vector control in the DU (nuclei outlined *hda-1(RNAi)* micrograph). Statistical significance determined through using an unpaired two sample t-test, with Welch's correction (*p ≤ 0.05; ***p ≤ 0.001; n.s., not significant). Scale bars: 5 µm.

Description

During *C. elegans* development, two cells, Z1 and Z4, give rise to the entire somatic gonad, including populations of dorsal uterine (DU) and ventral uterine (VU) cells, as well as the postmitotic anchor cell (AC), which invades the underlying basement membrane during uterine-vulval morphogenesis (Kimble & Hirsh, 1979; Sherwood & Sternberg, 2003). The helix-loop-helix transcription factor *hlh-2* (E/Daughterless) is expressed in these three cell types, among others, and is particularly enriched in the AC following post-transcriptional down-regulation of HLH-2 in the VU through dimerization-driven degradation (Karp & Greenwald, 2003; Sallee & Greenwald, 2015). At the L2 stage, HLH-2 regulates the Notch signaling event that specifies AC and VU fates, with its initial onset predicting the lineage ultimately giving rise to the presumptive VU (Karp & Greenwald, 2004; Attner *et al.*, 2019). Following AC/VU specification, HLH-2 functions to regulate cell cycle arrest and invasion of the AC (Medwig-Kinney *et al.*, 2020; Schindler & Sherwood, 2011). We and others have shown that HLH-2 does so by regulating expression of the nuclear hormone receptor and transcription factor NHR-67 (Tailless/TLX/NR2E1), and likely cell-cycle independent, pro-invasive targets as well (Bodofsky *et al.*, 2018; Medwig-Kinney *et al.*, 2020).

In addition to *hlh-2* and *nhr-67*, the histone deacetylase (HDAC) *hda-1* was also identified as a regulator of AC invasion through a reverse genetic screen (Matus *et al.*, 2010). It was later shown that *hda-1* function is necessary for AC invasive fate differentiation and plays a role in the pro-invasive pathway encompassing NHR-67 (Matus *et al.*, 2015). In order to further elucidate the mechanism by which HDA-1 regulates AC invasion, we sought to test we sought to test whether HDA-1 regulated expression of *hlh-2*. Previous studies of the *hlh-2* promoter identified a proximal regulatory element (*hlh-2(prox)*) that confers expression in the AC and VU cells specifically (**Figure 1A**) (Sallee & Greenwald, 2015). Approximately 3.3 kb downstream of this *hlh-2(prox)* element is an HDA-1 binding motif that lies within a putative HDA-1 binding site based on ChIP-sequencing data generated by the modENCODE Project (**Figure 1A**) (Shao *et al.*, 2020; Celniker *et al.*, 2009). Using CRISPR/Cas9 genome engineering, we edited the endogenous *hlh-2* locus to introduce a deletion mutation (*hlh-2(bmd231)*) from 1303 to 702 base pairs (bp) upstream of the GFP start codon, hereafter referred to as *hlh-2(Δ-1303-702)* (**Figure 1A**).

Consistent with findings using immunostaining, we find that endogenous GFP::*hlh-2* expression is normally enriched in the AC compared to the VU and DU (Karp & Greenwald, 2003) (**Figure 1B**). When compared to wild type, the *hlh-2(Δ-1303-702)* mutant showed a modest but statistically significant reduction in HLH-2 expression in the AC and VU cells (**Figure 1C-D**). The endogenous GFP::*hlh-2* allele paired with high resolution microscopy allowed us to detect subtle regulation of HLH-2 expression by *hda-1* in the AC and VU cells that was not previously reported using a transgenic reporter (Ranawade *et al.*, 2013). DU expression, however, was virtually eliminated in the mutant when accounting for camera-derived background noise (**Figure 1C-D**). We also observed that cytoplasmic expression of HLH-2 in the AC was modestly reduced in the mutant as well (**Figure D-E**). However, the alterations in HLH-2 expression in the AC and VU do not seem to be functionally significant, as expression of a NHR-67, a downstream target of HLH-2 in the cell cycle dependent pro-invasive gene regulatory network (Medwig-Kinney *et al.,* 2020), was not significantly reduced (**Figure 1F-G**). Furthermore, no defects in AC specification or invasion were observed in any of the strains containing the *hlh-2(Δ-1303-702)* allele (n > 50) based on both the presence of a single AC and an underlying gap in the basement membrane, in all animals examined (visualized by *cdh-3p*::mCherry::moeABD and laminin::GFP, respectively). RNAi-induced knockdown of *hda-1* resulted in reduced levels of HLH-2 in the DU, providing further evidence of this regulatory interaction (**Figure 1H-I**).

In summary, here we generate and characterize a new mutant allele of *hlh-2*. Deletion of the genomic region containing a putative HDA-1 binding site from the *hlh-2* promoter appears to primarily affect expression in the DU cells and is recapitulated through RNAi-induced knockdown of *hda-1*. Although HDA-1 is traditionally thought of as a repressor of transcription through chromatin deacetylation (Kadosh & Struhl, 1997; Kadosh & Struhl, 1998; Rundlett *et al.*, 1998; Gui *et al.*, 2003), this data adds to the growing evidence that HDACs can also function as activators of transcription (Vidal & Gaber, 1991; De Nadal *et al.*, 2004; Wang *et al.*, 2014). Whether there is a functional consequence of *hlh-2* depletion in the DU cells

is currently unknown. It is our hope that this reagent will be useful to the *C. elegans* community to further study the roles of *hda-1* and *hlh-2*.

Methods

[Request a detailed protocol](#)

Strain maintenance:

Animals were reared under standard conditions and cultured at 25°C (Brenner, 1974). Animals were synchronized through alkaline hypochlorite treatment of gravid adults to isolate eggs (Porta-de-la-Riva *et al.*, 2012). The RNAi clone targeting *hda-1* was generated by cloning 923 bp of cDNA (available from wormbase.org; Harris *et al.*, 2020) into the highly efficient T444T RNAi feeding vector (Sturm *et al.*, 2018). RNAi experiments were performed by feeding synchronized L1s following hypochlorite treatment.

CRISPR/Cas9 injections:

In order to generate the deletion mutation in the *hlh-2(Δ-1303-702)* allele, Cas9 protein injections were performed as previously described (Paix *et al.*, 2014; Ghanta *et al.*, 2020) with minor modifications to the published protocols. In short, a 200 bp ssODN donor repair ultramer for *hlh-2* (IDT) was constructed. To facilitate easy screening of our edit, a PvuI restriction site was engineered into the ssODN repair oligo as previously described (Paix *et al.*, 2014), flanked on each side by 94 bp of sequence homologous to the region surrounding the putative HDA-1 binding site. Single guide RNAs for *hlh-2* and *dpy-10* (co-CRISPR marker) were purchased from CRISPRevolution by Synthego (Synthego Corporation). The Cas9/sgRNA ribonucleoprotein complex was formed by incubating 30 pmols of Cas9 NLS protein (California Institute for Quantitative Biosciences at UC Berkeley (QB3-Berkeley)) with 23.75 pmoles of each *hlh-2* gRNA, and 47.5 pmoles of *dpy-10* sgRNA for 15 minutes at 37°C. The *hlh-2* and *dpy-10* ssODN donor repair ultramers (IDT) were then added to the reaction at a final concentration of 2.2 µg.

TagRFP-T::AID was inserted into the C-terminus of the endogenous *nhr-67* locus via CRISPR/Cas9 mediated genome engineering using the self-excising cassette method (Dickinson *et al.*, 2013; Dickinson *et al.*, 2015). The sgRNA targeting sequence in pDD122 was replaced with the sgRNA targeting the C-terminus of *nhr-67* using Gibson cloning (Dickinson *et al.*, 2013). The repair template for *nhr-67* was generated by cloning homology arms, synthesized by Twist Biosciences (left homology arm) and by PCR using genomic DNA as a template (right homology arm), into pTNM063 (TagRFP-T::AID repair template) (Ashley *et al.*, 2021).

Live cell imaging:

Micrographs were collected on a Hamamatsu Orca EM-CCD camera mounted on an upright Zeiss AxioImager A2 with a Borealis-modified CSU10 Yokagawa spinning disk scan head (Nobska Imaging) using 488 nm and 561 nm Vortran lasers in a VersaLase merge and a Plan-Apochromat 100×/1.4 (NA) Oil DIC objective. MetaMorph software (Molecular Devices) was used for microscopy automation. Animals were mounted into a drop of M9 on a 5% Noble agar pad containing approximately 10 mM sodium azide anesthetic and topped with a coverslip.

Image quantification:

Images were processed using Fiji/ImageJ (v.2.0.0) (Schindelin *et al.*, 2012). Nuclear expression of HLH-2 and NHR-67 was quantified by measuring mean gray value as previously described (Medwig-Kinney *et al.*, 2020). DU and VU cells were sampled by selecting the three most proximal to the AC and closest to the coverslip. Cytoplasmic expression of HLH-2 was measured using the freehand selection tool, tracing the outline of the cell but excluding the nucleus. For all quantification, background subtraction was performed by subtracting the mean gray value of a background region of an equal area to account for EM-CCD camera noise.

Data visualization and statistical analysis:

Representative micrographs were processed using Fiji/ImageJ and assembled into figures using Adobe Illustrator (v.23.0.6). RStudio (v.1.4.1717) was used to generate violin/sina plots and to perform statistical analyses.

Reagents

Strains:

Strain	Genotype	Source

DQM350	*hlh-2*(bmd90[*hlh-2p*::LoxP::GFP::HLH-2]) I; *qyIs225*[*cdh-3p*::mCherry::moeABD] V; *qyIs7*[laminin::GFP] X.	Medwig-Kinney *et al.,* (2020)
DQM704	*nhr-67*(bmd212[*nhr-67p*::NHR-67::TagRFP-T::AID]) IV; *hlh-2(bmd90[hlh-2p*::LoxP::GFP::HLH-2]) I.	This study
DQM785	*hlh-2(bmd231[hlh-2p(Δ-1303-702)*>LoxP::GFP::HLH-2]) I; *qyIs225*[*cdh-3p*::mCherry::moeABD] V; *qyIs7*[laminin::GFP] X.	This study
DQM900	*hlh-2(bmd231[hlh-2p(Δ-1303-702)*::LoxP::GFP::HLH-2]) I; *nhr-67*(bmd212[*nhr-67p*::NHR-67::TagRFP-T::AID]) IV.	This study

Sequences:

Reagent	Sequence
dpy-10 sgRNA	GCUACCAUAGGCACCACGAG + Synthego modified EZ Scaffold
dpy-10 ssODN	CACTTGAACTTCAATACGGCAAGATGAGAATGACTGGAAACCGTACCGCATGCGGTGCCTATGGTAGCGGAGCTTCACATGGCTTCAGACCAACAGCCTAT
hda-1(RNAi) targeting sequence	TTGATGGAGCACGGTAAGCGCCGTGTCGCCTACTACTATGACTCCAACATTGGAAATTACTATTATGGTCAAGGGCACGTCATGAAGCCACATCGTATCAGAATGACCCATCATCTCGTTCTCAACTATGGTCTGTACCGGAATTTAGAGATTTTCCGCCCATTCCCTGCATCATTCGAAGACATGACTCGTTTTCACAGCGACGAGTACATGACGTTTTTGAAGAGTGCGAATCCAGATAATCTGAAATCCTTCAACAAACAAATGCTTAAGTTCAATGTTGGAGAAGATTGTCCTCTCTTTGATGGTCTTTATGAGTTCTGCCAACTCAGTTCGGGAGGTTCTCTGGCTGCTGCCACTAAATTGAACAAGCAGAAGGTGGACATTGCTATCAATTGGATGGGAGGCCTCCATCACGCCAAGAAAAGCGAGGCGTCCGGATTCTGTTACACCAATGACATCGTTCTCGGTATTCTCGAGCTTCTCAAGTACCACAAGCGAGTACTTTACGTCGATATTGATGTTCATCACGGAGATGGAGTAGAGGAGGCGTTCTATACGACTGATCGAGTAATGACAGTGTCATTCCATAAATATGGAGATTTCTTCCCAGGAACCGGAGACCTGAAAGATATAGGAGCTGGAAAAGGAAAGCTCTATTCAGTCAATGTTCCACTTCGCGATGGAATCACCGACGTCTCTTACCAGAGTATTTTTAAACCAATCATGACAAAGGTTATGGAGAGATTTGATCCCTGTGCTGTTGTTCTTCAATGTGGAGCTGATTCTCTCAACGGAGATAGACTTGGACCATTCAATCTGACCTTGAAAGGCCACGGAGAATGTGCTCGTTTCTTCCGAAGCTACAACGTTCCACTTATGATGGTCGGTGGAGGTGGATACACTCCAAGAAATGTGGCACG
hlh-2 (-1303 bp) gRNA	AUGAAUGUACUCCCUACAGU + Synthego modified EZ Scaffold
hlh-2 (-702 bp) gRNA	UAAGGAUUCGUAAACAUUGU+ Synthego modified EZ Scaffold

hlh-2(Δ-1303-702) ssODN	CTCTCACTCTTACCATATTCTGAAGAATTAAAAATTTCAGAGATCCCTACAAAACTCTAATAACATGCTTCAAAAATGAATGTACTCCCTACAGTCGATCGTAATAGACAATGTTTACGAATCCTTACCAATTTTGAATTTAAACAAGAACGCAAATGTATTGTAGGGCAGTTTTTTTTTCAATTATTGAGTTTATCAAAA
nhr-67 C-terminus sgRNA	AGAGAGTGTTAATGTTGAAG
nhr-67 C-terminus left homology arm	GGAATAATGTGAGACTTCACTATAAAGGTAAACGCTGTTTTTCTGAGTGGGTTGCAACGATCAAAGTTAATTAAATATTGTATTTGCTAGTTTGAAGGTTGCTAATTCTTTTTTAAAATTAATTAATTAACCAATTGAAAAAGTTCATTTATAGTTTTTGTACGATTATCCTATTCAAAAGTTCATTTTTCGGCTCAAAATATAAAAAATTCCACAATTAAAAAAGCAGTGTTTTTTGTTCTCACAAAAAATGCAAATTATTTCCTATTTGCTTAAAAAGCGAAATTGATTATTGAAAACTAATGAAAACTAAACGCTCTAGTACCATCTTTCCTTCTGAAAACTTCACAGTCTGAAACCTATTTCAGATGTATAAATGCAATTGCCGCTATTCCAACAACTTCAATAATTGATGTTCTATTCCGCCCTTCAATTGGATCAGCTTCAATGCCAAGACTTATTCAAGACATGTTCAAGCCACCACAACAACCCACTCCTACGTCACTGTTTCCAATGGCAAACTTCAATTTGAACTTTCTATTAAAACAAGAAAAAACCGAAACTGAAGAGGGTGAAGATATTGAAGAAGAGGATGATGCGACGAGTAGCAATCAATTTGATGAAAATTCTTCTACTGATGATAGGTATGATGAGCATTTATTAGTACAGTGGATTAACTGAGTCTGTTGCAGATCTGTCGGAGAACTGGATCCCGTTCAACTTTTCTTGGCTCTTAATTCCTCAACTCAGCCTTCATCGGCATCATCCCCTTCCTCTTCAAGACCACGTCATTCGATTCGATCAATAACTGAATTATTATCAATTCAAGAAGAGGAAAGCGTGAACGTGGAGGAAGTG
nhr-67 C-terminus right homology arm	TAAATAGTAAATTCATGTTTCATATACAGTAACTCAATTATTCTAAGTATCTCTTTTCATTGTCTTTTTCACTCCGTTTCTTGCCTCGCCCGGATTTTCATTGGATTTTGATTTATACTTTCAAAATTTCATTTTTCAATTGTAAATTTTTAATTTAAATTTAGAGAAAAAAAATGGTAAGCTTTAAAACTAATTTATTATTTTCTGATTTATATTGTGAACAGATGAATAAAACGTTTACAACAATGGCAATTGGCATACAAACATCATTAAAAAAAGGTGAATCATACAGTTTTGAGAAGACTACATATGATTCGAAACATAAAAAACAATAGAAATCAATAAATGATGGGAGAGAAACCGAGAGATTTATTGGAAAATGGAACGGTTGAATGTCATATTGTGTCATCGTCGTTTTCCTTGTTAATGGCCTCGTTTCTTATCATATCCATATCATTCTGATATTCCCATTCAACTAGATGACCAAATCATTAGCTGACTGATTTCCCCCTTTTTAATGATTTGTTTATGGTTTTGTCAATAGTTTGAACGCGTTACGTTTTTGTAGATAAACCTGATTATGCTAGAATATTTTTTATTGAGATTTATTGACTAATTTAAAGTTTTAAACTAACAGAACAACAACCAATATTATAAAGAAAATGCTTTAAACTCATTTTTGAACATCCAGAACATCCGAAAAATAACCAACATGGTTAAGATTTTTCAAAGTTTTTAGTCAAAGTTTCGGTATCTATTTGCAATTTTCAAAAAACATGGAATATTTTCAGTAATTGCTTTTTCGAACTCCCAGACTGTTTGAATACAAAAATTGAAAAGCAAGTAAACAATAAAAAATTGTAGATATTTTTTCAAAGACTTTCAAAATTATAGGCGTAGGCTTCACTAATTTTTGACTGTCAGTAAAATATTTATTTCAAAAAAATTTTAAAAGTTTTACCATAATATTTGGGCATGGGCATTTTACTTTTAAAAACGATTTCTAAAGAAACCATTTTTATATGTAAAACAGTTTTGCTCAATTTTACCAGTTATCAA

Forward primer to amplify *nhr-67* C-terminus right homology arm from gDNA	CGGCGGCGTTCGTGAAATAAATAGTAAATTCATGTTTCATATAC
Reverse primer to amplify *nhr-67* C-terminus right homology arm from gDNA	GCTATGACCATGTTATCGATTTCCTAGTTGATAACTGGTAAAATTGAGCA

References

Ashley GE, Duong T, Levenson MT, Martinez MAQ, Johnson LC, Hibshman JD, Saeger HN, Palmisano NJ, Doonan R, Martinez-Mendez R, Davidson BR, Zhang W, Ragle JM, Medwig-Kinney TN, Sirota SS, Goldstein B, Matus DQ, Dickinson DJ, Reiner DJ, Ward JD. 2021. An expanded auxin-inducible degron toolkit for *Caenorhabditis elegans*. Genetics 217: iyab006. PMID: 33677541.

Attner MA, Keil W, Benavidez JM, Greenwald I. 2019. HLH-2/E2A Expression Links Stochastic and Deterministic Elements of a Cell Fate Decision during *C. elegans* Gonadogenesis. Curr Biol 29: 3094-3100.e4. PMID: 31402303.

Bodofsky S, Liberatore K, Pioppo L, Lapadula D, Thompson L, Birnbaum S, McClung G, Kartik A, Clever S, Wightman B. 2018. A tissue-specific enhancer of the *C. elegans* nhr-67/tailless gene drives coordinated expression in uterine stem cells and the differentiated anchor cell. Gene Expr Patterns 30: 71-81. PMID: 30404043.

Brenner S. 1974. The genetics of *Caenorhabditis elegans*. Genetics 77: 71-94. PMID: 4366476.

Celniker SE, Dillon LA, Gerstein MB, Gunsalus KC, Henikoff S, Karpen GH, Kellis M, Lai EC, Lieb JD, MacAlpine DM, Micklem G, Piano F, Snyder M, Stein L, White KP, Waterston RH, modENCODE Consortium. 2009. Unlocking the secrets of the genome. Nature 459: 927-30. PMID: 19536255.

De Nadal E, Zapater M, Alepuz PM, Sumoy L, Mas G, Posas F. 2004. The MAPK Hog1 recruits Rpd3 histone deacetylase to activate osmoresponsive genes. Nature 427: 370-4. PMID: 14737171.

Dickinson DJ, Ward JD, Reiner DJ, Goldstein B. 2013. Engineering the *Caenorhabditis elegans* genome using Cas9-triggered homologous recombination. Nat Methods 10: 1028-34. PMID: 23995389.

Dickinson DJ, Pani AM, Heppert JK, Higgins CD, Goldstein B. 2015. Streamlined Genome Engineering with a Self-Excising Drug Selection Cassette. Genetics 200: 1035-49. PMID: 26044593.

Ghanta KS, Mello CC. 2020. Melting dsDNA Donor Molecules Greatly Improves Precision Genome Editing in *Caenorhabditis elegans*. Genetics 216: 643-650. PMID: 32963112.

Gui CY, Ngo L, Xu WS, Richon VM, Marks PA. 2004. Histone deacetylase (HDAC) inhibitor activation of p21WAF1 involves changes in promoter-associated proteins, including HDAC1. Proc Natl Acad Sci U S A 101: 1241-6. PMID: 14734806.

Harris TW, Arnaboldi V, Cain S, Chan J, Chen WJ, Cho J, Davis P, Gao S, Grove CA, Kishore R, Lee RYN, Muller HM, Nakamura C, Nuin P, Paulini M, Raciti D, Rodgers FH, Russell M, Schindelman G, Auken KV, Wang Q, Williams G, Wright AJ, Yook K, Howe KL, Schedl T, Stein L, Sternberg PW. 2020. WormBase: a modern Model Organism Information Resource. Nucleic Acids Res 48: D762-D767. PMID: 31642470.

Kadosh D, Struhl K. 1997. Repression by Ume6 involves recruitment of a complex containing Sin3 corepressor and Rpd3 histone deacetylase to target promoters. Cell 89: 365-71. PMID: 9150136.

Kadosh D, Struhl K. 1998. Histone deacetylase activity of Rpd3 is important for transcriptional repression in vivo. Genes Dev 12: 797-805. PMID: 9512514.

Karp X, Greenwald I. 2003. Post-transcriptional regulation of the E/Daughterless ortholog HLH-2, negative feedback, and birth order bias during the AC/VU decision in *C. elegans*. Genes Dev 17: 3100-11. PMID: 14701877.

Karp X, Greenwald I. 2004. Multiple roles for the E/Daughterless ortholog HLH-2 during *C. elegans* gonadogenesis. Dev Biol 272: 460-9. PMID: 15282161.

Kimble J, Hirsh D. 1979. The postembryonic cell lineages of the hermaphrodite and male gonads in *Caenorhabditis elegans*. Dev Biol 70: 396-417. PMID: 478167.

Matus DQ, Li XY, Durbin S, Agarwal D, Chi Q, Weiss SJ, Sherwood DR. 2010. In vivo identification of regulators of cell invasion across basement membranes. Sci Signal 3: ra35. PMID: 20442418.

Matus DQ, Lohmer LL, Kelley LC, Schindler AJ, Kohrman AQ, Barkoulas M, Zhang W, Chi Q, Sherwood DR. 2015. Invasive Cell Fate Requires G1 Cell-Cycle Arrest and Histone Deacetylase-Mediated Changes in Gene Expression. Dev Cell 35: 162-74. PMID: 26506306.

Medwig-Kinney TN, Smith JJ, Palmisano NJ, Tank S, Zhang W, Matus DQ. 2020. A developmental gene regulatory network for *C. elegans* anchor cell invasion. Development 147: dev185850. PMID: 31806663.

Paix A, Wang Y, Smith HE, Lee CY, Calidas D, Lu T, Smith J, Schmidt H, Krause MW, Seydoux G. 2014. Scalable and versatile genome editing using linear DNAs with microhomology to Cas9 Sites in *Caenorhabditis elegans*. Genetics 198: 1347-56. PMID: 25249454.

Porta-de-la-Riva M, Fontrodona L, Villanueva A, Cerón J. 2012. Basic *Caenorhabditis elegans* methods: synchronization and observation. J Vis Exp 64: e4019. PMID: 22710399.

Ranawade AV, Cumbo P, Gupta BP. 2013. *Caenorhabditis elegans* histone deacetylase hda-1 is required for morphogenesis of the vulva and LIN-12/Notch-mediated specification of uterine cell fates. G3 (Bethesda) 3: 1363-74. PMID: 23797102.

Rundlett SE, Carmen AA, Suka N, Turner BM, Grunstein M. 1998. Transcriptional repression by UME6 involves deacetylation of lysine 5 of histone H4 by RPD3. Nature 392: 831-5. PMID: 9572144.

Sallee MD, Greenwald I. 2015. Dimerization-driven degradation of *C. elegans* and human E proteins. Genes Dev 29: 1356-61. PMID: 26159995.

Schindler AJ, Sherwood DR. 2011. The transcription factor HLH-2/E/Daughterless regulates anchor cell invasion across basement membrane in *C. elegans*. Dev Biol 357: 380-91. PMID: 21784067.

Schindelin J, Arganda-Carreras I, Frise E, Kaynig V, Longair M, Pietzsch T, Preibisch S, Rueden C, Saalfeld S, Schmid B, Tinevez JY, White DJ, Hartenstein V, Eliceiri K, Tomancak P, Cardona A. 2012. Fiji: an open-source platform for biological-image analysis. Nat Methods 9: 676-82. PMID: 22743772.

Shao LW, Peng Q, Dong M, Gao K, Li Y, Li Y, Li CY, Liu Y. 2020. Histone deacetylase HDA-1 modulates mitochondrial stress response and longevity. Nat Commun 11: 4639. PMID: 32934238.

Sherwood DR, Sternberg PW. 2003. Anchor cell invasion into the vulval epithelium in *C. elegans*. Dev Cell 5: 21-31. PMID: 12852849.

Sturm Á, Saskoi É, Tibor K, Weinhardt N, Vellai T. 2018. Highly efficient RNAi and Cas9-based auto-cloning systems for *C. elegans* research. Nucleic Acids Res 46: e105. PMID: 29924347.

Vidal M, Gaber RF. 1991. RPD3 encodes a second factor required to achieve maximum positive and negative transcriptional states in *Saccharomyces cerevisiae*. Mol Cell Biol 11: 6317-27. PMID: 1944291.

Wang Z, Lyu J, Wang F, Miao C, Nan Z, Zhang J, Xi Y, Zhou Q, Yang X, Ge W. 2018. The histone deacetylase HDAC1 positively regulates Notch signaling during *Drosophila* wing development. Biol Open 7: bio029637. PMID: 29437043.

Author Contributions: Taylor N Medwig-Kinney: Conceptualization, Formal analysis, Investigation, Resources, Visualization, Writing - original draft. Nicholas J Palmisano: Formal analysis, Conceptualization, Investigation, Resources,

Writing - review and editing. David Q Matus: Conceptualization, Funding acquisition, Project administration, Supervision, Writing - review and editing.

Reviewed By: Anonymous

History: Received August 13, 2021 **Revision received** August 24, 2021 **Accepted** August 25, 2021 **Published** September 2, 2021